doi:10.1093/brain/aww119 BRAIN 2016: 139; 1971–1986 | 1971

BRAIN
A JOURNAL OF NEUROLOGY

Migraine photophobia originating in cone-driven retinal pathways

Rodrigo Noseda,[1,2] Carolyn A. Bernstein,[1,2] Rony-Reuven Nir,[3] Alice J. Lee,[4] Anne B. Fulton,[2,5] Suzanne M. Bertisch,[2,6] Alexandra Hovaguimian,[2,7] Dean M. Cestari,[2,8] Rodrigo Saavedra-Walker,[1] David Borsook,[2,9] Bruce L. Doran,[10] Catherine Buettner[2,6] and Rami Burstein[1,2]

Migraine headache is uniquely exacerbated by light. Using psychophysical assessments in patients with normal eyesight we found that green light exacerbates migraine headache significantly less than white, blue, amber or red lights. To delineate mechanisms, we used electroretinography and visual evoked potential recording in patients, and multi-unit recording of dura- and light-sensitive thalamic neurons in rats to show that green activates cone-driven retinal pathways to a lesser extent than white, blue and red; that thalamic neurons are most responsive to blue and least responsive to green; and that cortical responses to green are significantly smaller than those generated by blue, amber and red lights. These findings suggest that patients' experience with colour and migraine photophobia could originate in cone-driven retinal pathways, fine-tuned in relay thalamic neurons outside the main visual pathway, and preserved by the cortex. Additionally, the findings provide substrate for the soothing effects of green light.

1 Department of Anesthesia, Critical Care and Pain Medicine, Beth Israel Deaconess Medical Center, Boston MA 02215, USA
2 Harvard Medical School, Boston, MA 02115, USA
3 Department of Neurology, Rambam Health Care Campus, and Laboratory of Clinical Neurophysiology, Faculty of Medicine, Technion - Israel Institute of Technology, Haifa, Israel, 31096
4 Harvard Catalyst Clinical Research Center, Beth Israel Deaconess Medical Center, Boston, MA 02215, USA
5 Department of Ophthalmology, Children's Hospital Boston, Boston MA 02115, USA
6 Department of Medicine, Beth Israel Deaconess Medical Center, Boston, MA 02215, USA
7 Department of Neurology, Beth Israel Deaconess Medical Center, Boston, MA 02215, USA
8 Department of Neuro-ophthalmology, Massachusetts Eye and Ear Infirmary, Boston, MA 02114, USA
9 Center for Pain and the Brain, Department of Anesthesia Critical Care and Pain Medicine, Boston Children's Hospital, Boston, MA 02115, USA
10 Diagnosys LLC, Lowell, MA 01854, USA

Correspondence to: Rami Burstein,
CLS-649, 330 Brookline Avenue,
Boston, MA 02215,
USA
E-mail: rburstei@bidmc.harvard.edu

Keywords: headache; thalamus; electroretinography; visual evoked potential; pain

Abbreviations: ERG = electroretinography; LP = lateral posterior thalamic nucleus; Po = posterior thalamic nucleus; VPM = ventral posteromedial thalamic nucleus

Received January 7, 2016. Revised March 28, 2016. Accepted April 3, 2016. Advance Access publication May 17, 2016

Introduction

Exacerbation of headache by light (photophobia) is commonly associated with intracranial pathologies such as migraine, meningitis, concussion, and subarachnoid haemorrhage (Welty and Horner, 1990; Lamonte *et al.*, 1995; Aurora *et al.*, 1999; Kawasaki and Purvin, 2002). It is experienced by ~80% of migraineurs with normal eyesight (Liveing, 1873; Selby and Lance, 1960; Drummond, 1986; Choi *et al.*, 2009). Although not as incapacitating as the headache, photophobia renders migraineurs dysfunctional as they are forced to halt fundamental daily tasks to seek the comfort of darkness. Because of the frequency of attacks, migraineurs endure a substantial burden that interferes with work and home life.

Attempting to understand how light exacerbates migraine headache, we reported that photic signals that originate in intrinsically photosensitive retinal ganglion cells containing melanopsin, a photoreceptor with peak sensitivity to blue light (Lucas *et al.*, 2001; Berson *et al.*, 2002; Hattar *et al.*, 2003), converge on thalamic trigeminovascular neurons believed to relay nociceptive signals from the dura to the cortex during migraine (Noseda *et al.*, 2010). Consequently, we suggested that this 'non-image forming' pathway might explain the preferential sensitivity to blue light in blind migraine patients, who, in spite of losing the ability to form images due to degeneration of cones and rods, can detect light (Noseda *et al.*, 2010).

Based on our data as well as earlier observations made in subjects lacking the outer retina (Zaidi *et al.*, 2007), an impression was created that blue light could be fundamental to migraine-type photophobia and that the exacerbation of the headache by light could be minimized by devices (sunglasses, contact lens) that block the blue light (Good *et al.*, 1991; Main *et al.*, 2000; Adams *et al.*, 2006; Blackburn *et al.*, 2009). Although this notion was generated by observations made in blind migraineurs lacking cones and rods (Zaidi *et al.*, 2007), rather than in migraineurs with normal eyesight, it raised the question of whether colours can modulate headache intensity differently in migraineurs whose retinas contain functioning cones and rods.

Materials and methods

All study visits took place at Beth Israel Deaconess Medical Center (BIDMC), Boston, MA (September 2010 to May 2015). The BIDMC Committee on Clinical Investigations approved the study and all participants provided written informed consent. Patients were recruited from the BIDMC Comprehensive Headache Center, Neurology clinic, and the primary care clinic and from advertisements at the Medical Center and Harvard Medical School. Subjects aged 15–85 years old were potentially eligible for the study if they met the International Classification of Headache Disorders Committee (2013) criteria for migraine with or without aura, were able to communicate in English and were willing to attend a visit during an untreated migraine attack. Exclusion criteria included fewer than five headache-free days per month, chronic head or neck pain not attributed to migraine, chronic use of opioids ($\geqslant$15 days/month for three previous consecutive months or longer), or having an ocular disease. For this study an ocular disease was defined as a primary and persisting visual disorder, including anterior chamber of the eye disease (such as glaucoma), macular degeneration, retinal degenerative diseases, cones dystrophy, rods dystrophy, achromatopsia (colour blindness, i.e. either totally colourblind or almost totally colourblind), retinitis pigmentosa, Leber's congenital amaurosis, albinism, night blindness, or cortical blindness due to posterior circulation stroke. Participants were permitted to stop the study or any phase of testing at any time.

Psychophysical studies assessing patients' sensitivity to different colours of light during migraine

The study included 69 migraine patients. Of these, 41 completed the psychophysical assessments during migraine. Assessments included the effects that different colours of light had on the: (i) intensity of their headache; (ii) throbbing; (iii) muscle tenderness; and (iv) cephalic areas affected by the pain. These assessments were made during untreated migraine attacks. Prior to testing, patients were allowed to sit in a dimly lit room for 20 min. The light was then turned off for 3 min and patients were asked to verbally rate their headache intensity on a scale of 0–10, outline its location (e.g. in, behind and around the eyes, in the forehead, temple, top of the head, back of the head, on one side or on both), and indicate whether the headache throbbed and whether their neck muscles felt tender. Their answers at that time, prior to beginning of sensitivity-to-colour testing, were used to define their baseline. Once a baseline was established, participants were positioned in front of a full-field ganzfeld ColorDome (Diagnosys LLC), the light was turned on at the lowest intensity ($1\,cd{\cdot}m^{-2}$), and then increased incrementally (1, 5, 20, 50 and $100\,cd{\cdot}m^{-2}$) every 30 s. As a reference, $1\,cd{\cdot}m^{-2}$ provides a background light that is just above dark level whereas $100\,cd{\cdot}m^{-2}$ is equivalent to a normally lit office space. The first light was white, the second was blue (447 ± 10 nm), the third was green (530 ± 10 nm), the fourth was amber (590 ± 10 nm), and the fifth was red (627 ± 10 nm) (Supplementary Fig. 1). While looking at the light (full-field), they were asked to describe any change (worsening or improvement) in their headache intensity, appearance of headache in areas outside its original site, onset of throbbing (only in cases in which the headache did not throb at baseline), and onset of muscle tenderness (only in cases in which muscles did not feel tender at baseline). To reduce the number of variables, all participants underwent the same sequence of stimulation (white, blue, green, amber, red). To minimize additive effects, patients were allowed to sit in total darkness for 3 min between consecutive series of stimulation or as long as it took for their headache intensity, headache location, throbbing and muscle tenderness to return to their baseline level. Supporting the fact that the order of stimulation did not affect the results, were the following: (i) the least 'photophobic' green light was always presented after the highly 'photophobic' white and blue lights; and (ii), patients' rating of the headache when exposed to amber and red lights, which appear at the end of the order of stimulation, were similar to

their rating when exposed to white and blue lights, which appear at the beginning of the order of testing.

Electroretinography recording

Electroretinographies (ERGs) were recorded in 46/69 patients; three were excluded due to unreliable recording. As recommended by the International Society for Clinical Electrophysiology of Vision (McCulloch *et al.*, 2015) we used the full-field (ganzfeld) stimulation method as it increases recording stability, reproducibility and reliability by delivering the photic stimuli to all photoreceptors at a relatively homogenous manner. To minimize discomfort, the pupils were not dilated and the ERG recordings were not done through a contact lens electrode. Rather, all ERG recording were done using one disposable, low-impedance silver/nylon corneal recording electrode (DTL Plus) that is comfortable and easy to use, one reference gold cup electrode placed on the forehead, and a ground silver ear clip electrode placed on the ipsilateral ear. To ensure good ocular contact and proper electrode impedance, we first ran a few test stimuli to verify that the recorded waveforms were comparable to the standard ERG. Amplification of signals, fixation point and other technical aspects of our ERG recording, all provided technically by the same ColourDome used in the psychophysical studies, adhered to the guideline of 'Standard for clinical electroretinography' as defined in McCulloch *et al.* (2015).

Light-adapted, single-flash, cone electroretinography

Before recording cone ERG, patients were given 10 min to adapt to the background light. The stimulus intensity of each flash of light was 3.0 $cd \cdot s \cdot m^{-2}$ (calculated as time integrated luminance and measured in photopic candela-seconds per meter square), the duration was 4 ms, and the background luminance was 30 $cd \cdot m^{-2}$. At this background luminance, rods are saturated and do not respond to light increment or decrement (Hood and Finkelstein, 1986). Using these parameters, each colour of light was flashed nine times at a 1-s interval. The nine flashes of light were divided to three series; each averaged the ERG signals recorded over three flashes of light (Supplementary Fig. 2A). The order of colour stimuli was white, blue, green, amber and red. For comparisons, we measured a-wave amplitude (from baseline to trough), b-wave amplitude (from trough of a-wave to peak of b-wave) and the implicit time (from stimulus onset to peak b-wave) as described in Supplementary Fig. 2D.

Light-adapted 30 Hz flicker cone electroretinography

The 30 Hz flickering ERG consisted of 150 single flashes of light, delivered over a period of 5 s. At 30 Hz, rods do not contribute to the ERG signal as they cannot follow this speed (Dodt, 1951). As above, the intensity of each flash of light was 3.0 $cd \cdot s \cdot m^{-2}$, the duration was 4 ms, and the background illumination was 30 $cd \cdot m^{-2}$. Using these parameters, each patient was exposed to three series of 150 single flashes (29 ms interstimulus interval) per colour in the same order as above, and the average of the three series was used in the data analysis (Supplementary Fig. 2B). Because the first few ERGs could represent responses to a single flash, they were discarded. For comparisons, we measured a-wave amplitude (trough), b-wave amplitude (peak) and the implicit time as described in Supplementary Fig. 2D.

Dark-adapted rod electroretinography

Before recording the rod system ERG, patients were kept in total darkness for 20 min. To minimize detection by cones, dim flashes of light (0.01 $cd \cdot s \cdot m^{-2}$, 4 ms) were delivered in the absence of background illumination. As in the light-adapted flash ERG, each colour of light was flashed nine times at a 1.1-s interval. The nine flashes of light were divided into three series; each averaged the ERG signals recorded over three flashes of light (Supplementary Fig. 2C). As above, dark-adapted rod ERGs were repeated with white, blue, green, yellow and red lights. For comparisons, we measured b-wave amplitude and time to peak as described in Supplementary Fig. 2D.

Multi-unit recording in the rat thalamus

Animals and surgical procedures

Experiments were approved by the Beth Israel Deaconess Medical Center and Harvard Medical School standing committees on animal care, and conducted in accordance with the U.S. National Institutes of Health Guide for the Care and Use of Laboratory Animals. Twenty-five male Sprague-Dawley rats (250–350 g) were initially anaesthetized with a single dose of methohexital sodium (45 mg/kg intraperitoneally) for endotracheal intubation and cannulation of the right femoral vein. Rats were then mounted on a stereotaxic frame and connected to a gas anaesthesia system that delivers a mixture of isoflurane and oxygen at 100 ml/min. Surgical procedures were performed using 2.5% isoflurane, while the subsequent experimental protocol was carried out under 1–1.2% isoflurane. End-tidal CO_2, blood oxygen saturation, respiratory and heart rates, and core body temperature were continuously monitored and kept within physiological range throughout the experiment. Two craniotomies were performed. The first was drilled on the left side of the skull at the lambdoid suture to allow stimulation of the dura overlying the transverse sinus. A second craniotomy was made on the right side of the skull (~2.5 mm behind bregma; ~2.5 mm lateral to the midline) to access the posterior thalamic area for extracellular multi-site, multi-unit recording with tetrodes (see below) (Supplementary Fig. 3A). The exposed dura was kept moist using modified synthetic interstitial fluid (pH 7.2). Immobilization of animals during recordings was achieved by continuous intravenous infusion of a mixture of the muscle relaxants vecuronium (1 mg/ml) and rocuronium (5 mg/ml) in NaCl 0.9% at a rate of 1 ml/h (1:1).

In vivo electrophysiological recordings

Multi-unit extracellular recordings were performed using three quartz-insulated platinum/tungsten tetrodes (1–2 MΩ) mounted on a remote-controlled microdrive system equipped with a 12-channel low noise pre-amplifiers (Tetrode Mini Matrix, Thomas Recording). We used tetrodes instead of conventional microelectrodes as they increase the yield and reliability of single-unit isolation from multi-unit recordings (Gray *et al.*, 1995). All 12-channel continuous electrophysiological signals were amplified using a multichannel programmable gain main amplifier (PGMA, Thomas Recording). Data were acquired using an expanded Micro1401-mkII digitizer unit (CED) and sent to a PC

for additional post-acquisition processing (see signal processing below). Preliminary real-time waveform discrimination was performed for initial characterization of neuronal responses using Spike2 software (CED), and was based on template creation from spontaneous and evoked action potentials. The three tetrodes were independently lowered into the right posterior thalamus in search of neuronal discharges evoked by electrical pulses (0.8 ms, 0.5–3.0 mA, 1 Hz) applied on the exposed contralateral dura. If an isolated waveform corresponding to a single neuron exhibited discrete firing bouts in response to such electrical pulses, mechanical (calibrated von-Frey monofilament) and chemical (1 M KCl) stimulation of the dura were also applied to confirm the presence of at least one dura-sensitive neuron per experiment in the multi-unit signal. Once a dura-sensitive neuron was found, the recording tetrode remained in its position while attempts were made to find more such neurons with the other two independent tetrodes. When neuronal search was finalized, all three tetrodes remained in their final position for the rest of the experiment (see experimental design for details). At the end of the recording session, electrolytic lesions marking recording location of each tetrode were made by passing 10 µA direct current for 10 s with a stimulus generator connected to an integrated impedance/stimulation device (Thomas Recording). Subsequently, each rat was euthanized with an overdose of pentobarbital sodium (100 mg/kg intraperitoneally and perfused with 200 ml of saline), followed by 400 ml of a fixative solution [4% paraformaldehyde in phosphate-buffered saline (PBS)]. Brains were removed, soaked in 30% sucrose-PBS for 48 h, frozen, cut into coronal sections (80-µm thick) using a cryostat (Leica), and mounted on glass slides for imaging. Digital images of sections containing electrolytic lesions were obtained with epifluorescence microscopy (Leica) and superimposed over an atlas of the rat brain (Paxinos and Watson, 2008). Counterstaining with neutral red was also performed to confirm precisely anatomical location of each recording site.

Experimental design: neuronal classification and photic stimuli

Experiments were performed when stable recording of multi-unit activity was established in the three tetrodes over a resting period of 20–30 min. For *a posteriori* classification, neurons were tested for their responsiveness to the electrical, mechanical and chemical stimulation of the contralateral dura. Neurons responding to two of three modalities of dural stimulation were classified as dura-sensitive; neurons responding to fewer than two modalities were classified as dura-insensitive. Once classified, neurons were tested for their responses to photic stimuli. Prior to beginning of photic stimuli, the light was turned off for a period of 15 min. The colours-of-light stimulation paradigm (dark-light-dark, 1 min each) started at the end of the dark period (Supplementary Fig. 3B). Calibrated photic stimulation was delivered using a customized ColourBurst stimulator (Diagnosys LLC) positioned 1 cm from the cornea. White, blue, green and red lights were projected at the same order and same maximal intensity (100 $cd \cdot m^{-2}$) used in the human studies. A neuron was classified as light sensitive if it responded to at least one colour of light. A response was considered positive if a stimulus increased the firing rate over the baseline by >2 standard deviations (SD).

Signal processing: detection and sorting of spikes from individual neurons

The amplified 12-channel continuous electrophysiological signals were sampled at 30 kHz and filtered between 0.3 and 6 kHz. Offline, data were exported to Matlab® and processed for spike detection and sorting using Wave_clus algorithm (Quiroga *et al.*, 2004). Briefly, this algorithm combines new methods for setting amplitude thresholds for spike detection, the wavelet transform for spike features extraction with optimal resolution in both time and frequency domains, and superparamagnetic clustering for grouping spikes belonging to a single neuron. Manual adjustments of settings in the Wave_clus GUI were also used when the automatic clustering performed by the algorithm did not provide well-isolated clusters of single units. Once the units were satisfactorily isolated, data were sent to NeuroExplorer® for the evaluation of neuronal responses and construction of peri-stimulus histograms.

Visual evoked potential recording

Visual evoked potentials were recorded in 46/69 participants. Of these, only 28 yielded waveforms with clearly identifiable N1, P1, N2 and P2 deflections. As recommended by the International Society for Clinical Electrophysiology of Vision guideline for visual evoked potential standard (Odom *et al.*, 2010), we elicited full field light flashes using the ColorDome system. Recordings were made using gold-disc surface electrodes. The active electrode was placed on the scalp over the visual cortex (at point Oz); the reference electrode was placed over the forehead (at point Fz); the ground electrode was placed on the scalp over the vertex (at point Cz) (American Encephalographic Society, 1994). To establish colour-specific visual evoked potentials, patients were placed in a dimly illuminated room (non-dilated pupils), and presented with five sets of photic stimuli in the following order: white, blue, green, yellow and red. Each set of photic stimuli consisted of 64 flashes of light delivered at 1.1 Hz (frequency), 3.0 $cd \cdot s \cdot m^{-2}$ (intensity), 4 ms (duration). Analysis time was set at 300 ms. Because peaks of N2 and P2 waves are the most robust components of flash visual evoked potentials (Supplementary Fig. 4B), comparisons between visual evoked potential responses to white, blue, green, amber and red were based on their amplitudes and time to peak.

Calibration and quantification of photic stimulation

Repeated calibrations of our ColorDome with the international light technologies photometer (ILT1700) and an Ocean Optics Maya LSL spectrometer were used to verify that the different colours of light were delivered at equal luminance. For example, when the nominal luminance was set at 3 $cd \cdot m^{-2}$ in the Espion software (Diagnosys LLC), the measured luminance for blue, green, amber and red was 2.96, 3.0, 3.36, 2.76 $cd \cdot m^{-2}$, respectively. To ensure that each of these colours appeared to be exactly the same luminance to our participants (i.e. taking into account differences in photopic sensitivity of the human retina), our ColorDome delivered different power with each photic stimulus. When the measured luminance for blue, green, amber and red was 2.96, 3.0, 3.36, 2.76 $cd \cdot m^{-2}$, the respective power was 32.2, 1.9, 2.1, and 4.9 $\mu W/cm^2/nM$.

Statistical analysis

Detailed descriptions of all statistical analyses are included in the Supplementary material and in Supplementary Tables 1–6. Briefly, data from the psychophysical, ERG and visual evoked potential studies in migraineurs were analysed using Mixed Linear Models (MLM), and data from the animal studies of thalamic neurons were analysed using exact logistic regression analysis and Fisher's one-sample randomization (permutation) test. Statistical significance was set at $P < 0.05$.

Results

Sixty-nine patients diagnosed with migraine (The International Classification of Headache Disorders, 2013), photophobia, and no known ocular diseases, were studied. Their demographic and headache characteristics are shown in Table 1. They were 40 ± 12 years of age (mean $\pm$ SD), mostly female (91%), with migraine history of 19 ± 12 years. Their attacks lasted 56 ± 48 h, and were associated with aura (36%), moderate to severe headache intensity (97%), unilateral location (70%), pulsating quality (77%), nausea or vomiting (83%) and phonophobia (86%).

Psychophysical studies in migraineurs

To determine whether there is a colour preference to migraine-type photophobia, we assessed the effects of white and four different colours of light on: (i) proportion of migraine patients who reported changes in headache intensity; (ii) magnitude of change in pain rating; (iii) number of patients who report change in sensory perception other than headache intensity; and (iv) spread of headache from its original site. Specifically, in 41 patients undergoing acute migraine attack we assessed headache intensity, headache location, throbbing, and muscle tenderness at dark (baseline) and during exposure to five series of photic stimuli. Each series consisted of 3 min in total darkness, followed by an incremental increase in the intensity of white, blue, green, amber and red lights (see 'Materials and methods' section and Supplementary Fig. 1). At the end of each series, the light was turned off and subjects were given sufficient time for their headache intensity to return to baseline.

Proportion of migraine patients who reported changes in headache intensity

The proportion of patients reporting changes in pain severity when exposed to the different colours of light increased in accordance with the elevated intensities of light (Fig. 1A). At the highest intensity ($100\,cd{\cdot}m^{-2}$), nearly 80% of the patients demonstrated an intensification of headache; this was true for all colours except the green, which affected half that proportion of patients. Unexpectedly, exposure to green light reduced pain intensity in ~20% of the patients.

Magnitude of change in pain rating

As to response magnitude, the headache intensity also increased in accordance with light intensity augmentation, demonstrating a comparable change for all colours of light but green. The latter decreased pain perception more effectively at low (1 and $5\,cd{\cdot}m^{-2}$) than at medium (20, 50 and $100\,cd{\cdot}m^{-2}$) intensities (Fig. 1B). To determine the extent to which the different colours of light increased or decreased pain ratings, a separate analysis examined pain-rating differences only in trials in which exposure to light altered pain perception. At medium intensity, blue and red increased pain ratings by 18–19%, white and amber by 15%, whereas green increased the pain by <5% (Fig. 1C). Conversely, at low intensity, green light emerged as the only colour to induce a decrease in pain ratings; reduction was ~15%. Comparing the changes in headache severity in response to each colour of light at each intensity indicated that the response to green was significantly smaller as compared to all other colours in all intensity levels (Fig. 1D). As no interaction was found between the variables 'colour' and 'intensity' ($P = 0.735$), we concluded that the effect of 'colour' on change in pain intensity did not depend on the value of 'intensity'. Accordingly, the effect that each colour of light had on the change in pain rating (compared to baseline) was examined regardless of 'intensity' (i.e. all data per colour were pooled). This analysis showed that white, blue, amber and red induced a significant increase in pain ratings as compared to their baselines ($P < 0.0001$ for each comparison; Supplementary Table 1 and Fig. 1D); green was the only colour that did not demonstrate a significant change from the baseline pain ratings ($P = 0.7$; Supplementary Table 1 and Fig. 1D). A comparison between the different colours showed that green induced significantly smaller changes in pain ratings as compared to white, blue, amber and red ($P < 0.0001$ for each comparison), and that white evoked significantly smaller changes as compared to blue ($P = 0.002$), red ($P = 0.002$) and amber ($P = 0.03$). The remaining comparisons were insignificant (Supplementary Table 2).

Patients who report change in sensory perception other than headache intensity

Consistent with the findings above, blue, amber and red induced throbbing and muscle tenderness in more patients (40–50% for throbbing and 11–19% for muscle tenderness) than white and green (20–24% for throbbing and 8% for muscle tenderness) (Fig. 1E).

Spread of headache from its original site

Spread of headache is another dimension of photophobia demonstrating colour preference (Fig. 1F). Here again, more patients described spreading of headache when exposed to blue ($n = 19$), amber ($n = 17$) and red ($n = 21$) than to white ($n = 9$) and green ($n = 11$). Of those, ~25% reported spread of pain from front to back, and 35% reported that their headaches spread to the contralateral side.

Table 1 Characteristics of migraineurs

ID	Age	Sex	Years with migraine	Attacks/ month (*n*)[a]	CM versus EM	Visual aura	Usual duration w/o treatment (h)	Unilateral location	Pulsating quality	Usual pain intensity moderate or severe	Aggravated by physical activity	Nausea and/or vomiting	Phonohobia[b]
1	38	F	22	5	EM	MA	72	+	+	+	+	+	
2	49	F	37	6	EM	MA	72	+	+	+	+	+	+
3	38	F	23	3	EM	MO	72	+	+	+	+	+	+
4	27	F	17	9	EM	MA	18	+	+	+	+		+
5	49	F	28	4	EM	MO	72		+	+	+	+	+
6	37	F	27	8	EM	MA	72		+	+	+	+	+
7	30	F	9	5.5	EM	MA	⩾4			+			
8	46	F	9	1	EM	MA	72	+		+	+	+	+
9	17	M	15	2.5	EM	MO	120	+	+	+	+	+	+
10	47	F	26	>15	CM	MO	⩾4			+			
11	29	F	20	9	CM	MO	72	+	+	+	+	+	+
12	41	F	27	1	EM	MO	72		+	+	+	+	+
13	42	F	2	2.5	EM	MO	96	+	+	+	+	+	+
14	33	F	12	>15	CM	MO	⩾4			+			
15	39	F	19	2.5	EM	MO	72	+		+		+	+
16	46	F	28	12	CM	MA	48		+	+	+	+	+
17	49	F	41	4.5	EM	MO	24	+	+	+	+	+	+
18	47	F	26	12	CM	MO	⩾4			+		+	
19	53	F	15	30	CM	MO	24	+		+	+	+	+
20	42	M	13	12	CM	MO	15	+	+	+	+		+
21	24	F	14	0.5	EM	MO	72		+	+	+	+	+
22	39	F	23	10	EM	MA	⩾4		+	+		+	+
23	38	F	2	4	EM	MA	72			+	+	+	+
24	49	F	34	2	EM	MA	180	+	+	+	+	+	+
25	36	F	27	7	EM	MO	168	+		+		+	+
26	24	F	7	4	EM	MO	36	+	+	+	+		+
27	33	F	21	17.5	CM	MO	168	+	+	+	+	+	+
28	44	F	19	>15	CM	MO	24	+	+	+			+
29	41	F	15	>15	CM	MA	240	+	+	+	+	+	+
30	56	F	4	16	CM	MA	72	+	+	+	+	+	+
31	63	F	15.5	16	CM	MA	72	+	+	+	+	+	+
32	49	F	14	16	CM	MA	36	+	+	+	+	+	+
33	30	M	3	25	CM	MA	72		+	+	+	+	+
34	35	F	16	5.5	EM	MO	⩾4	+	+				+
35	29	F	2	8	EM	MO	24		+	+		+	+
36	52	F	27	9	EM	MO	24	+		+			+
37	29	F	11	20	CM	MA	8		+	+		+	+

(continued)

Table 1 Continued

ID	Age	Sex	Years with migraine	Attacks/ month (*n*)[a]	CM versus EM	Visual aura	Usual duration w/o treatment (h)	Unilateral location	Pulsating quality	Usual pain intensity moderate or severe	Aggravated by physical activity	Nausea and/or vomiting	Phonohobia[b]
38	62	M	54	8	EM	MO	48			+		+	+
39	46	F	26	15	CM	MO	72	+	+	+	+	+	+
40	28	F	10	6	EM	MO	72	+	+	+	+	+	
41	34	F	22	1.5	EM	MO	60	+	+	+	+		+
42	29	F	16	8	EM	MO	48		+			+	
43	34	F	19	9	EM	MA	48	+	+	+	+	+	+
44	57	F	7	1	EM	MO	168	+	+	+		+	+
45	50	F	20	8	EM	MO	72	+	+	+		+	+
46	49	F	19	4.5	EM	MO	168	+	+	+		+	+
47	22	F	4	9	EM	MA	8	+	+	+	+	+	+
48	53	F	36	1	EM	MO	24	+	+	+		+	+
49	44	F	32	4.5	EM	MO	24	+		+	+	+	+
50	47	M	24	4.5	EM	MO	72	+	+	+		+	
51	58	F	45	15	EM	MO	84	+	+	+	+	+	+
52	48	F	7	2.5	CM	MO	72			+	+	+	+
53	40	F	19	7	EM	MA	36		+	+			+
54	77	F	63	4	EM	MO	72	+	+	+	+	+	+
55	39	F	23	2.5	EM	MA	48	+	+	+	+	+	+
56	20	F	4	1	EM	MA	24	+	+	+	+	+	+
57	25	F	9	4	EM	MO	$\geqslant 4$	+	+	+	+	+	+
58	27	F	15	9	EM	MO	$\geqslant 4$	+	+	+	+	+	+
59	33	F	15	1.6	EM	MA	10	+	+	+	+	+	+
60	37	F	27	1.5	EM	MO	48	+		+	+	+	+
61	20	F	3	3	EM	MO	72	+	+	+	+	+	
62	34	F	9	2.5	EM	MA	48	+	+	+		+	
63	59	M	23	>15	EM	MO	$\geqslant 4$	+	+	+	+	+	+
64	26	F	16	2.5	CM	MA	24		+	+			+
65	55	F	16	5	EM	MA	72	+		+	+	+	+
66	33	F	25	2.5	EM	MA	72		+	+	+	+	+
67	28	F	17	8	EM	MO	4	+	+	+	+	+	+
68	23	F	2	1	EM	MA	10	+		+		+	+
69	26	F	5	2.5	EM	MA	6		+	+	+	+	+

CM = chronic migraine; EM = episodic migraine; MA = migraine with aura; MO = migraine without aura

[a]All participants were screened and confirmed by a study physician to have migraine according to the International Classification of Headache Disorders.

[b]All participants had photophobia as a criterion of inclusion to the study.

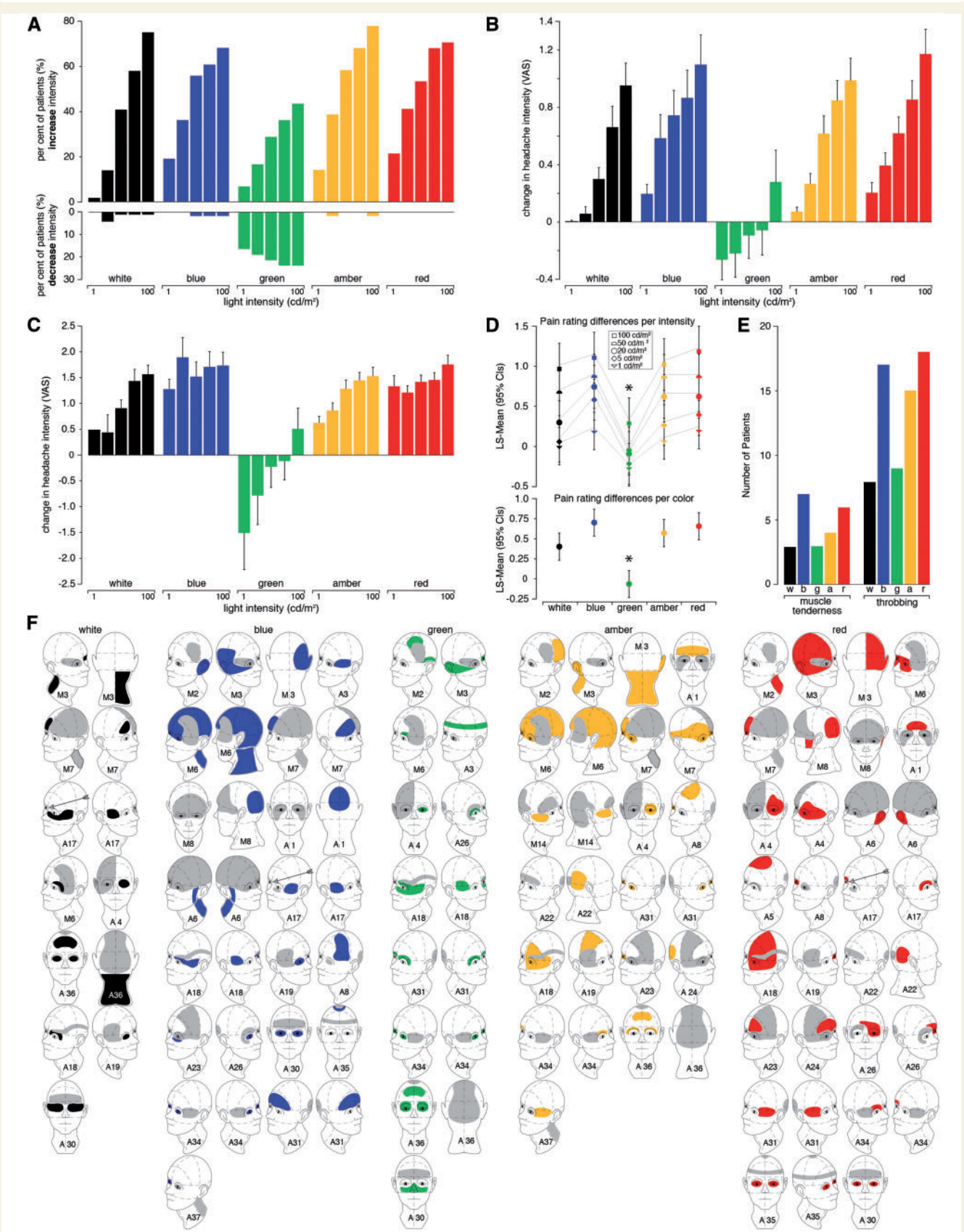

Figure 1 Effects of colour on pain ratings, throbbing, muscle tenderness and headache location. (**A**) Proportion of patients experiencing an increase or decrease in pain intensity when exposed to white, blue (447 ± 10 nm), green (530 ± 10 nm), amber (590 ± 10 nm) and red (627 ± 10 nm) lights; each presented for 30 s at low (1 and 5 cd·m^{-2}) and medium (20, 50 and 100 cd·m^{-2}) intensities. (**B**) Numerical

Electroretinography studies in migraineurs

To explain the psychophysical findings, we sought to determine whether electrical signal generated by the retina in response to green light differed from those generated by the other colours. To answer this question we studied 45 migraine patients when they were pain-free; 43 yielded reliable ERG waveforms. Each patient underwent (i) light-adapted single-flash cone ERG; (ii) light-adapted 30-Hz flicker cone ERG; and (iii) dark-adapted rod ERG, as recommended by the International Society for Clinical Electrophysiology of Vision (ISCEV; McCulloch *et al.*, 2015). Each ISCEV ERG condition was done with white and then repeated with blue, green, amber and red (See 'Materials and methods' section and Supplementary Fig. 2).

In light-adapted single-flash cone ERG, b-wave amplitude [calculated from trough to peak; expressed as median (95% confidence interval); Fig. 2A, D and G] generated by green light [99.78 μV (87 to 111.51)] was significantly smaller ($P < 0.001$) than the blue [119.54 μV (110.52 to 130.51)] and white [105.9 μV (98.21 to 119.83)] amplitudes but similar to the amber [94.14 μV (85.29 to 104.46)] and red [97.42 μV (93.51 to 107.97)] amplitudes (Supplementary Table 3). The significantly larger blue b-wave amplitude (compared to all other colours, $P < 0.001$ for each comparison) stemmed from greater a-wave amplitude [−43.03 μV (−46.52 to −38.85); all others from −27.54 μV (−30.18 to −21.54) to −24.97 μV (−31.26 to −22.95); Fig. 2A, D, G and Supplementary Table 3].

In contrast, in the light-adapted flicker cone ERG (Fig. 2B, E and H), the b-wave amplitude generated by green light [64.77 μV (56.24 to 70.26)] was significantly smaller ($P < 0.003$) than that generated by blue [83.41 μV (73.75 to 91.31)], red [71.69 μV (66.82 to 74.76)], and white [69.15 μV (62.04 to 77.52)] (Supplementary Table 4). As above, the significantly smaller b-amplitude derived from the a-wave (Fig. 2B, E, H and Supplementary Table 4).

In the dark-adapted rod ERG , the b-wave amplitude generated by green light was significantly smaller than those generated by blue and white, and significantly larger than those generated by amber and red (Fig. 2C, F, I and Supplementary Table 5).

Collectively, these ERGs suggest that activation of cone-mediated (but not rod) retinal pathways can play a role in the weak 'photophobic' effects of green and strong 'photophobic' effects of white, blue and red.

Multi-unit recording of responses to different colours of light in the rat thalamus

To determine how differences in cone responses to blue, white and green lights are processed by thalamic neurons that constitute the second limb of the retino-thalamo-cortical pathway for exacerbation of headache by light (Noseda *et al.*, 2010), we recorded simultaneously from dura-sensitive, dura-insensitive, light-sensitive and light-insensitive neurons in lateral posterior (LP), posterior (Po) and ventral posteromedial (VPM) nuclei. The stimulation paradigm included mechanical stimulation of the dura in a dimly lit room, followed by 15 min of darkness for establishing baseline activity, and then four stimulation cycles (dark-light-dark, 1-min each) in the same order (white-blue-green-red) and at the same maximal value of intensity (100 $cd \cdot m^{-2}$) used in the human psychophysical studies (Supplementary Fig. 3).

In six experiments we were successful in simultaneously recording and isolating 97 thalamic neurons. Of these, 24 were dura-sensitive (10 Po, eight LP, six VPM), 73 dura-insensitive (27 Po, 25 LP, 21 VPM), 37 light-sensitive (13 Po, 20 LP, four VPM), and 60 light-insensitive (24 Po, 13 LP, 23 VPM) (Fig. 3A and B). These 97 neurons were exposed to 140 stimulation cycles of white, 249 stimulation cycles of blue, 188 stimulation cycles of green, and 192 stimulation cycles of red (Fig. 4A, C and E). Analysis of firing frequency [mean spikes/s ± standard error of the mean (SEM)] recorded in all 97 neurons during the 769 stimulation cycles showed that exposure to blue and white lights significantly increased neuronal activity (blue, from 1.07 ± 0.12 to 1.58 ± 0.16 spikes/s, $P < 0.0001$, $n = 249$; white, from 1.29 ± 0.19 to 1.71 ± 0.29 spikes/s $P = 0.011$, $n = 140$), whereas exposure to green light did not (green, from 1.13 ± 0.17 to 1.29 ± 0.17 spikes/s, $P = 0.395$, $n = 188$)—adding mechanistic support to the clinical observation that green light is least likely to induce

Figure 1 Continued

change in headache intensity (mean ± SEM) reported by all patients in response to each colour and intensity (VAS = verbal analogue scale). (**C**) Bar graphs showing only those trials in which lights altered pain perception. Note that all colours but green increased pain ratings by a maximum of 15–20% (0–10 VAS), whereas green—the only colour to decrease pain ratings—attenuated the pain by a maximum of 15%. (**D**) Pain rating differences (from baseline) grew larger with increasing stimulus intensity, such that differences in response to green light were significantly smaller as compared to all other colours at all intensities (*top*, mean ± 95% CI). Analysed regardless of stimulus intensity (colour-intensity interaction was statistically insignificant), all colours but green demonstrated a significant increase in pain ratings compared to baseline (*bottom*, $P < 0.0001$ for each colour). (**E**) Number of patients who experienced muscle tenderness and throbbing during exposure to light compared to no such perception at baseline. (**F**) Effect of colours on spread of headache from its original location (grey areas). Cases in which the headache affected both sides of the head or the front and the back are illustrated in two images. Numbers represent individual patients. Arrows indicate directionality of the pain. w = white; b = blue; g = green; a = amber; r = red.

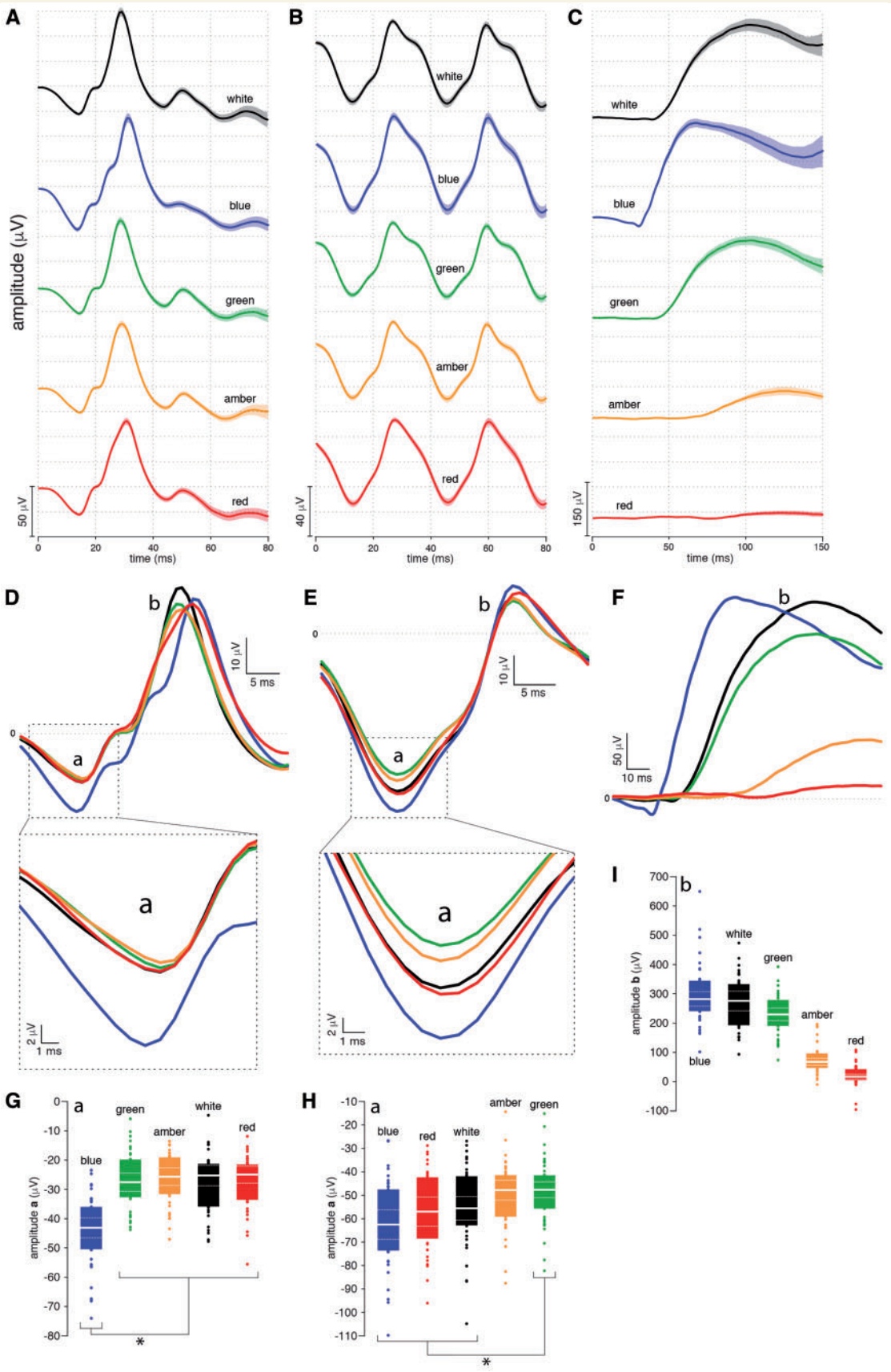

Figure 2 Chromatic electroretinographies (ERGs) recorded interictally in 43 migraine patients. (**A**) Standard light-adapted single flash ERG waveforms averaged (± SEM) across patients in response to 387 flashes (nine flashes per patient) of each colour of light. (**B**) Standard

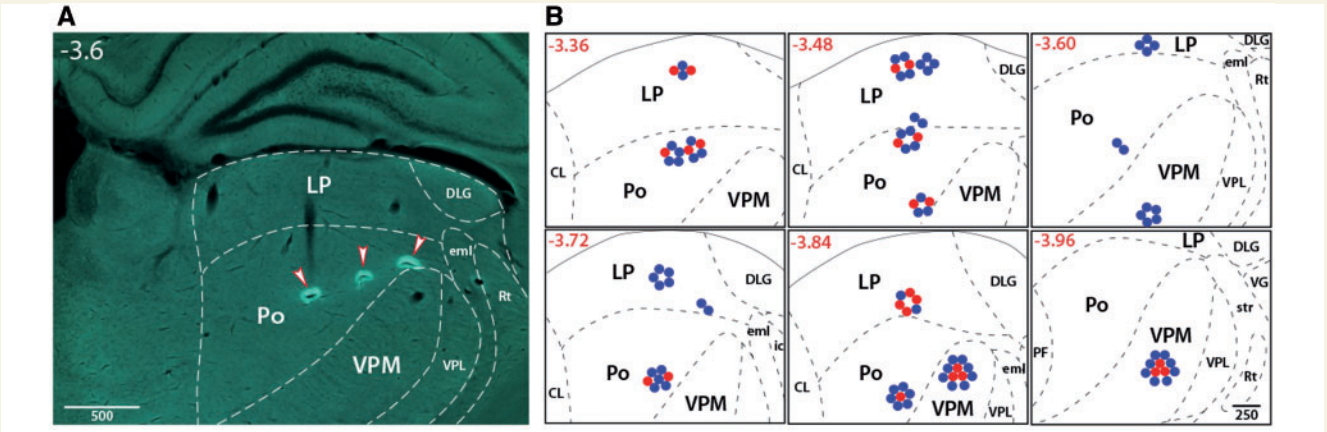

Figure 3 Recording sites of thalamic dura-sensitive and dura-insensitive neurons. (**A**) Lesions marking locations of three tetrodes used in one multi-unit, multi-site recording session. (**B**) Recordings were obtained simultaneously from dura-sensitive (red dots) and dura-insensitive (blue dots) neurons in the thalamic LP, Po and VPM nuclei. The number of dots surrounding each site depicts the number of single units isolated at that site. Numbers in upper left corners depict distance from bregma. CL = centrolateral thalamic nucleus; DLG = dorsolateral geniculate nucleus; eml = external medullary lamina; ic = internal capsule; Rt = reticular thalamic nucleus; str = stria terminalis; VG = ventral geniculate nucleus; VPL = ventroposterior lateral thalamic nucleus.

'photophobic' responses (Fig. 4). Because red light did not activate thalamic neurons (red, from 1.18 ± 0.15 to 1.16 ± 0.15 spikes/s, $P = 0.486$, $n = 192$), we excluded trials with red light from further analyses.

Analysis of responses to white, blue and green in each of the three thalamic nuclei revealed significant sensitivity to these colours of light in LP (from 1.69 ± 0.26 to 2.33 ± 0.3 spikes/s, $P < 0.0001$, $n = 181$) and Po (from 1.35 ± 0.1 to 1.86 ± 0.19 spikes/s, $P = 0.025$, $n = 177$), but not in VPM (from 0.53 ± 0.04 to 0.57 ± 0.04 spikes/s, $P = 0.138$, $n = 219$) (Fig. 4B, D, F and G). Because no colour of light significantly increased the response magnitude of VPM neurons (white, from 0.32 ± 0.07 to 0.38 ± 0.07; blue, from 0.64 ± 0.07 to 0.7 ± 0.07; green, from 0.46 ± 0.06 to 0.45 ± 0.06; red, from 0.6 ± 0.07 to 0.49 ± 0.06 spikes/s), they were excluded from further analyses (Fig. 4E–J).

Comparisons between responses to blue, green and white within LP and within Po, which was based on firing frequency analysis of 92 stimulation cycles recorded in the light-sensitive neurons, showed that the response to blue light was significantly larger than the response to green light in both LP ($P = 0.019$) and Po ($P = 0.042$), and significantly larger than the response to white light in LP ($P = 0.046$) but not in Po ($P = 0.461$) (Fig. 4H). The analysis also showed that the response to white light was significantly larger than the response to green light in Po ($P = 0.006$) but not in LP ($P = 0.850$) (Fig. 4H).

Dura-sensitive neurons demonstrated a significantly greater (2–3-fold) response probability to white [$P = 0.013$, odds ratio (OR) = 4.60], blue ($P = 0.002$, OR = 4.61) and green ($P = 0.023$, OR = 3.56) lights, as compared to dura-insensitive neurons (Fig. 4I). Among the dura-sensitive neurons, those located in LP demonstrated a significantly greater (2–3-fold) response probability to blue, as compared to those located in Po ($P = 0.023$, OR = 12.20) (Fig. 4J). Further demonstrating the likelihood that dura-sensitive LP neurons mediate the aversion to blue light is the finding that within LP, all dura-sensitive neurons responded to blue, but only half responded to white, and about a third to green (Fig. 4J). In contrast, the probability of neuronal response to white and green were comparable in these two nuclei (white: $P = 0.7$, OR = 2.22, green: $P = 1.0$, OR = 1.37).

Figure 2 Continued

light-adapted 30 Hz flickering ERG waveforms averaged (± SEM) across patients in response to each colour of light. (**C**) Standard dark-adapted rod ERG waveforms averaged (± SEM) across patients in response to each colour of light. (**D**) Superimposed means of light-adapted single flash ERG waveforms demonstrated that blue light generated significantly larger a-wave amplitude (enlarged view at *bottom*) as compared to all other colours ($P < 0.0001$). (**E**) Superimposed means of light-adapted 30 Hz flickering ERG waveforms show that blue, red and white lights generated significantly larger a-wave amplitudes as compared to green light ($P < 0.0001$). (**F**) Superimposed means of dark-adapted rod ERG waveforms show that the b-wave amplitudes generated by blue, white and green lights are significantly larger than those induced by amber and red. (**G**) Boxplot illustrating median (thick horizontal white line), 95% CI (thin dotted horizontal lines), interquartile range (25th–75th percentile; lower and upper box boundaries) and observations below and above the 25th and 75th percentile, respectively (individual dots). Asterisk depicts the significantly greater a-wave amplitude induced by the blue light compared to all other colours. (**H**) Boxplot illustrating median, 95% CI, interquartile range, and observations below and above the 25th and 75th percentile, respectively. Asterisks depict the significantly greater a-wave amplitude induced by blue, red and white lights compared to green. (**I**) Boxplot illustrating median, 95% CI, 25th to 75th percentile, and observations below and above 25th and 75th percentiles.

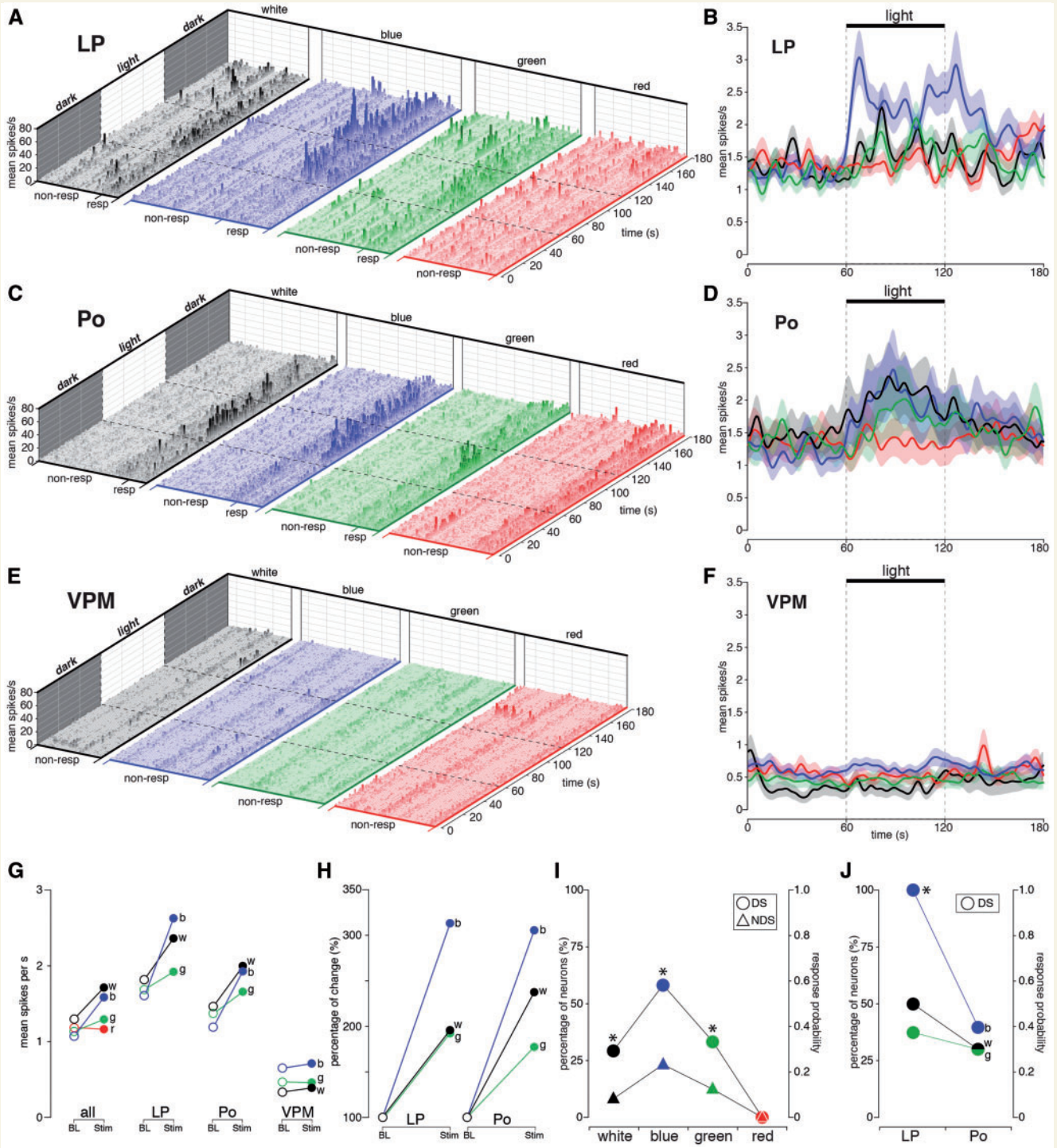

Figure 4 Differential responses of thalamic LP, Po and VPM neurons to photic stimulation with white, blue, green and red lights. (**A**) 3D bar graphs illustrating firing frequency (i.e. raw data expressed in mean spikes/s, bin size = 1 s) of all 33 LP neurons to 44, 76, 58 and 50 cycles (dark-light-dark, 1-min each) of photic stimulation with white, blue, green and red lights, respectively. Neurons whose activity in the light increased by >2 SD over baseline (i.e. in the dark), are marked as responders (resp) and shown on the right side of each collections of colour-selective bar graphs. (**B**) Graphs illustrating averaged responses (continuous line) ± SEM (shadowed area) of all 33 LP neurons to stimulation of the retina with white, blue, green and red lights. (**C**) 3D bar graphs illustrating firing frequency of all 37 Po neurons to 59, 58, 59, and 57 cycles of retinal stimulation with white, blue, green and red lights, respectively. (**D**) Graphs illustrating averaged responses (± SEM) of all 37 Po neurons to stimulation of the retina with white, blue, green and red lights. (**E**) 3D bar graphs illustrating lack of responses of the 27 VPM neurons to 35, 54, 58 and 55 cycles of retinal stimulation with white, blue, green and red lights, respectively. (**F**) Graphs illustrating averaged firing (± SEM) recorded in all 27 VPM neurons before, during and after stimulation of the retina with white, blue, green and red lights. Dotted lines in **A**–**F** depict onset and offset of photic stimulation. (**G**) Scatter plots summarizing response magnitude (mean spikes/s) of all neurons, and of neurons located in LP, Po and VPM, to photic stimulation with white, blue, green and red lights. BL = baseline firing in the dark; St = firing during light stimuli. (**H**) Per cent

Visual evoked potential studies in migraineurs

As perceptions of pain, light and colour are created in the cortex, we also sought to determine whether the psychophysical findings that (i) green evoked the least 'photophobic' responses; and (ii) blue, amber and red elicited the most 'photophobic' responses, could be expressed in the magnitude of the activity recorded in the cortex. To address these questions, the same 43 patients who underwent ERGs, underwent a standard flash visual evoked potential (Odom *et al.*, 2010), first with white light and then with blue, green, amber and red (see 'Materials and methods' section and Supplementary Fig. 4). Of these, only 28 patients yielded reliable and reproducible visual evoked potential signals (further explanation in methods). Analysis of the P2 amplitude values (median ± 95% CI), measured from 0 to P2 peak, based on 8960 flashes of light recorded successfully in 28 patients (28 × 5 colours × 64 flashes of each colour) revealed that green [11.14 μV (9.09 to 12.76)] was significantly smaller than blue [14.2 μV (11.36 to 17.24), $P = 0.016$], red [13.51 μV (9.54 to 17.48), $P = 0.02$], and amber [15.54 μV (10.28 to 18.12), $P = 0.002$] (Fig. 5A–C and Supplementary Table 6). In contrast, N2 amplitude values showed no significant differences (Supplementary Table 6). Reassuring the validity of the visual evoked potential recording were the findings that the median N2 and P2 latencies of the different colours of light were similar (ranging between 77.79 and 79.87 ms for N2, and between 114.4 and 117.3 ms for P2; $P > 0.05$, Supplementary Table 6).

Discussion

The study reveals a mechanism for the novel finding that exposure to green light exacerbates migraine headache significantly less than exposure to white, blue, amber or red lights in patients with normal eyesight. Taking into consideration results of ERG, thalamic and visual evoked potential recordings, the findings suggest that migraine photophobia may originate in the retina and fine-tuned in the thalamus, rather than in the cortex—a major shift in current thinking. Mechanistically, the psychophysical findings are explained by the differential responses of cone-driven retinal pathways, light-sensitive thalamic neurons in two sensory nuclei outside the main visual pathway, and the cortex to the different colours. Therapeutically, filtering out all but green light may prove beneficial for the reduction of photophobia and potentially the headache intensity.

To the best of our knowledge, this is the first study to compare the impact that different colours of light have on headache intensity in migraineurs undergoing acute migraine attacks. It is also the first study to use a technology that allows photic stimuli to be delivered at a narrow band of wavelengths and a single luminous intensity ($cd \cdot s \cdot m^{-2}$). Outside migraine attacks, Main and colleagues (2000) reported that the discomfort threshold of migraineurs is lower when exposed to low (380–530 nm) and high (580–730 nm) compared to medium (430–630 nm) wavelength of lights, and Good *et al.* (1991) found that glasses that filter blue light reduce migraine frequency (but not sensitivity to light) in children. These studies, although carried out interictally, and with far less precision regarding the range of wavelengths allowed in each of the three stimuli, support the findings that migraineurs are more sensitive to blue and red, as compared to green light.

Exploring potential mechanisms for colour preference, we first sought to determine whether the relative amplitude of the signals that the retina generates in response to each of the colours could be the cause of this phenomenon. Using the standard light-adapted single flash and flickering ERG paradigms (McCulloch *et al.*, 2015), we found that the a-wave amplitude generated by green light was smaller than the a-wave amplitude generated by blue, red and white lights, and that the a-wave amplitude generated by blue light was significantly larger than the a-wave amplitude generated by white, green, amber and red. Because, in the light-adapted flash ERG, the negative deflection of the a-wave originates from activation of cones (Brown and Wiesel, 1961*a*, *b*; Brown and Murakami, 1964; Penn and Hagins, 1969) and the peak and positive deflection reflect activity in ON- and OFF-bipolar and horizontal cells in the post-receptor retina (Miller and Dowling, 1970; Newman, 1980; Fulton and Hansen, 1988; Shirato *et al.*, 2008; Abd-El-Barr *et al.*, 2009; Miura *et al.*, 2009; Robson and Frishman, 2014), we propose that photophobia could originate in cone-driven retinal pathways—at the very beginning of the newly described non-image-forming visual pathway for exacerbation of headache by light (Noseda *et al.*, 2010, 2011). Because the a-wave discussed above was recorded under conditions that saturate the rod

Figure 4 Continued

change in firing frequency of all light-sensitive LP and Po neurons responding to blue, white and green lights. (**I**) Logistic regression analysis showing that compared to dura-insensitive neurons, dura-sensitive neurons are two to three times more likely (response probability) to respond to the different colours of light. (**J**) Exact logistic regression demonstrating that the probability of responses of dura-sensitive neurons to blue light is twice as high in LP as compared to Po. Within LP, the probability of response to blue light was twice as high as those recorded in response to white and green lights. Asterisks in **I** and **J** depict statistically significant ($P < 0.05$) differences between dura-sensitive and dura-insensitive neurons (**I**) and between responses to blue versus responses to white and green (**J**). w = white; b = blue; g = green; r = red.

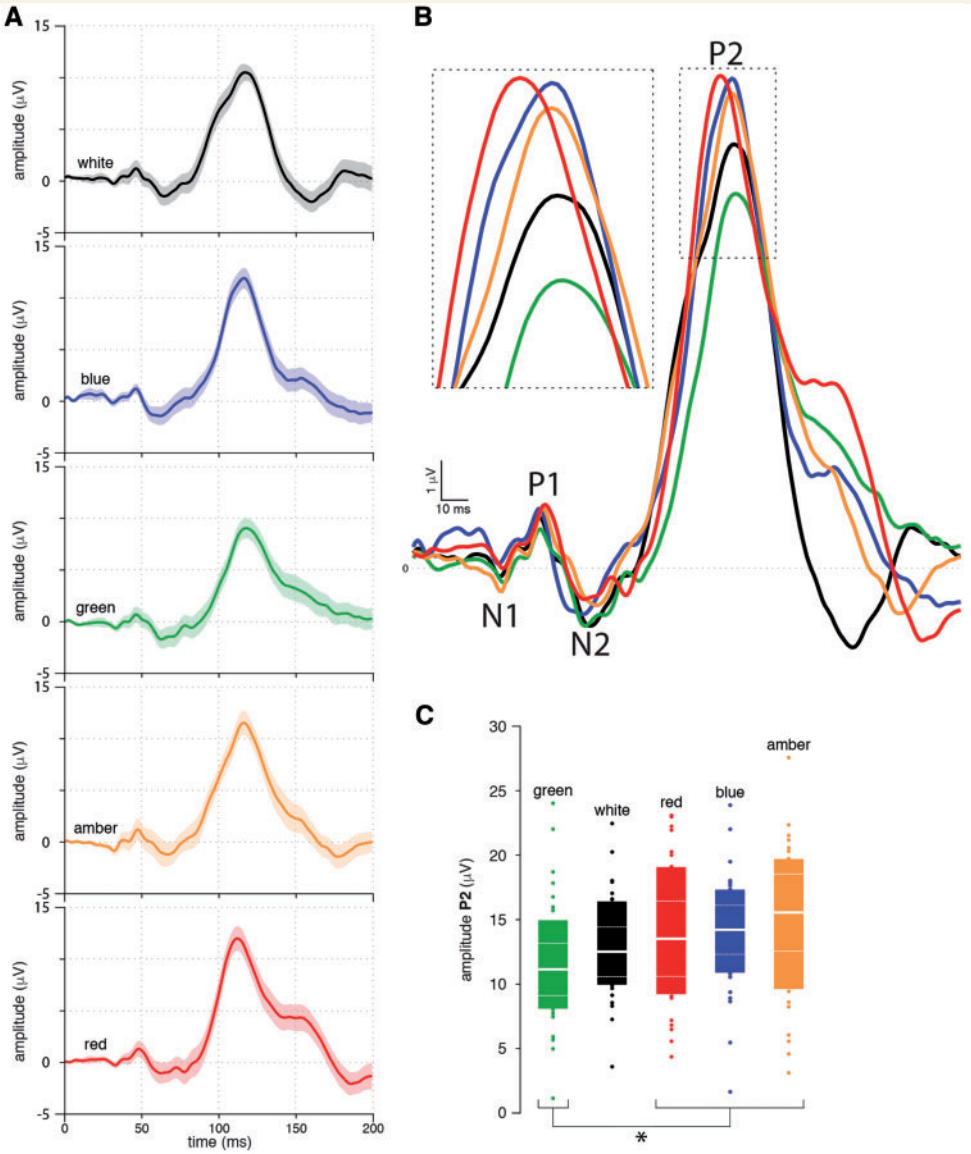

Figure 5 Chromatic VEPs recorded interictally in 28 migraine patients. (**A**) Standard flash visual evoked potential waveforms averaged (± SEM) across patients in response to 1792 flashes (64 flashes per patient, 1 s interstimulus interval) of each colour of light. The VEPs to flash stimulation consists of a series of negative and positive waves, the most robust of which are the N2 and P2 peaks. (**B**) Superimposed means of these flash VEPs demonstrated that blue, red and amber generated significantly larger P2 amplitude (enlarged view in inset) as compared to green ($P < 0.02$). In contrast, no differences were found in the amplitudes of the N2 waves. (**C**) Boxplot illustrating median (thick horizontal white line), 95% CI (thin dotted horizontal lines), interquartile range (25th–75th percentile; lower and upper box boundaries) and observations below and above the 25th and 75th percentile, respectively (individual dots). Asterisk depicts the significantly smaller P2-wave amplitude induced by the green light compared to red, blue and amber.

system (background illumination) (Hood and Finkelstein, 1986) and at frequency that was too fast for rods to follow (>28 Hz) (Dodt, 1951; Conner and MacLeod, 1977), we concluded that rods are unlikely to contribute to the 'photophobic' experience.

In line with our recently-described retino-thalamo-cortical pathway for migraine-type photophobia (Noseda *et al.*, 2010), we then determined whether the response magnitudes and firing probability of light-sensitive thalamic neurons in LP and Po (which constitute the 'thalamo' portion of the pathway) reflect or alter the different signals they receive from the retina, and whether their response characteristics could help explain why green light is least photophobic. Our simultaneous recording of multiple neurons in the three thalamic nuclei revealed that green generated the smallest responses in LP and Po, that blue generated the largest response in LP but not in Po, that white generated responses that are smaller than blue in LP and larger than green in Po, that VPM neurons are generally non-responsive to light, and that compared to dura-insensitive

neurons, dura-sensitive neurons are two to three times more likely to respond to light. Although we cannot comment on responses to red and amber lights, these findings establish the principle that the 'most photophobic' blue light activates more neurons and generates a greater magnitude of response than the 'least photophobic' green light and that white light, which is more 'photophobic' than green (and potentially less aversive than blue), activates neurons more robustly than green but less robustly than blue. Mechanistically, the findings suggest that both LP and Po neurons mediate the non-aversive reaction to green, that LP and to a lesser extent Po mediate the preferential aversion to blue, and that the distinction between white and green occurs in Po.

Finally, as human perception is established in the cortex, we also determined whether the magnitude of the electrical signals generated in the cortex by the different colours of light correlates with the subjective perception that green is less 'photophobic' than blue, amber, red and white; the distinguishably small ERG signals induced by green; and the relatively weak ability of green light to induce firing in the thalamic neurons. Using the standard flash visual evoked potential (Odom *et al.*, 2010), we found that the P2 amplitude generated by green was significantly smaller than the amplitudes generated by blue, amber and red. What prompted us to consider the P2 deflection as a meaningful response was the observation that regardless of the colour of light, it appeared stable across the 64 trials. At face value, these results can explain migraineurs' perception that green light is the least photophobic. However, as the neural source of the P2 deflection is unknown (Mehta *et al.*, 2000*a*, *b*), caution must be practiced in interpreting the findings. In the context of our study, there seems to be agreement that the P2 originates in the parieto-occipital region (Freunberger *et al.*, 2007), that it represents higher-order perceptual processing, and that it reflects complex neural processes that occur when a visual input is compared with an internal representation and stored memory (Luck and Hillyard, 1994; Evans and Federmeier, 2007; Freunberger *et al.*, 2007).

While the presented data are compelling, suggestions that cortical processing of photophobia may differ in classical versus common migraine (Cucchiara *et al.*, 2015) call attention to the need to repeat this study paradigm in different subpopulations of migraineurs, (i.e. episodic, chronic, with aura, without aura, in post-traumatic headache, etc.). Insufficient number of patients limited our ability to perform such comparisons in the current study. Along this line, it may also be interesting to determine effects of the stimulation paradigms used in this study on healthy control subjects.

In conclusion, this study demonstrates that green light is least likely to exacerbate migraine headache and that at low intensities it may even be therapeutic by reducing the headache intensity. The soothing effects of green are likely to involve a complex psychobiology (Hurlbert and Ling, 2007; Palmer and Schloss, 2010; Strauss *et al.*, 2013). Mechanistically, we propose that migraine photophobia can originate in cone-driven retinal pathways and is relayed through light-sensitive trigeminovascular thalamic neurons to the cortex, where patients' perception is highly correlated with the P2 waveform of the visual evoked potential.

Funding

This research was supported by NIH grants R37 NS079678, RO1 NS069847 (R.B.), R21 NS090254-02 (R.N.) and K24 NS77895 (D.B.). This work was conducted with support from Harvard Catalyst, The Harvard Clinical and Translational Science Center (National Center for Research Resources and the National Center for Advancing Translational Sciences, National Institutes of Health Award UL1 TR001102) and financial contributions from Harvard University and its affiliated academic healthcare centres. The funding sources had no involvement in the study design; collection, analysis, and interpretation of data; the writing of the report; and the decision to submit the article for publication. The content is solely the responsibility of the authors and does not necessarily represent the official views of Harvard Catalyst, Harvard University and its affiliated academic health care centres, or the National Institutes of Health.

Supplementary material

Supplementary material is available at *Brain* online.

References

Abd-El-Barr MM, Pennesi ME, Saszik SM, Barrow AJ, Lem J, Bramblett DE, et al. Genetic dissection of rod and cone pathways in the dark-adapted mouse retina. J Neurophysiol 2009; 102: 1945–55.

Adams WH, Digre KB, Patel BC, Anderson RL, Warner JE, Katz BJ. The evaluation of light sensitivity in benign essential blepharospasm. Am J Ophthalmol 2006; 142: 82–7.

American Encephalographic Society: Guideline for standard electrode position nomenclature. J Clin Neurophysiol 1994; 11(Guideline 13): 111–3.

Aurora SK, Cao Y, Bowyer SM, Welch KM. The occipital cortex is hyperexcitable in migraine: experimental evidence. Headache 1999; 39: 469–76.

Berson DM, Dunn FA, Takao M. Phototransduction by retinal ganglion cells that set the circadian clock. Science 2002; 295: 1070–3.

Blackburn MK, Lamb RD, Digre KB, Smith AG, Warner JE, McClane RW, et al. FL-41 tint improves blink frequency, light sensitivity, and functional limitations in patients with benign essential blepharospasm. Ophthalmology 2009; 116: 997–1001.

Brown KT, Murakami M. Biphasic form of the early receptor potential of the monkey retina. Nature 1964; 204: 739–40.

Brown KT, Wiesel TN. Analysis of the intraretinal electroretinogram in the intact cat eye. J Physiol 1961a; 158: 229–56.

Brown KT, Wiesel TN. Localization of origins of electroretinogram components by intraretinal recording in the intact cat eye. J Physiol 1961b; 158: 257–80.

Choi JY, Oh K, Kim BJ, Chung CS, Koh SB, Park KW. Usefulness of a photophobia questionnaire in patients with migraine. Cephalalgia 2009; 29: 953–9.

Conner JD, MacLeod DI. Rod photoreceptors detect rapid flicker. Science 1977; 195: 698–9.
Cucchiara B, Datta R, Aguirre GK, Idoko KE, Detre J. Measurement of visual sensitivity in migraine: validation of two scales and correlation with visual cortex activation. Cephalalgia 2015; 35: 585–92.
Dodt E. Cone electroretinography by flicker. Nature 1951; 168: 738.
Drummond PD. A quantitative assessment of photophobia in migraine and tension headache. Headache 1986; 26: 465–9.
Evans KM, Federmeier KD. The memory that's right and the memory that's left: event-related potentials reveal hemispheric asymmetries in the encoding and retention of verbal information. Neuropsychologia 2007; 45: 1777–90.
Freunberger R, Klimesch W, Doppelmayr M, Holler Y. Visual P2 component is related to theta phase-locking. Neurosci Lett 2007; 426: 181–6.
Fulton AB, Hansen RM. Scotopic stimulus/response relations of the B-wave of the electroretinogram. Doc Ophthalmol 1988; 68: 293–304.
Good PA, Taylor RH, Mortimer MJ. The use of tinted glasses in childhood migraine. Headache 1991; 31: 533–6.
Gray CM, Maldonado PE, Wilson M, McNaughton B. Tetrodes markedly improve the reliability and yield of multiple single-unit isolation from multi-unit recordings in cat striate cortex. J Neurosci Methods 1995; 63: 43–54.
Hattar S, Lucas RJ, Mrosovsky N, Thompson S, Douglas RH, Hankins MW, et al. Melanopsin and rod-cone photoreceptive systems account for all major accessory visual functions in mice. Nature 2003; 424: 76–81.
Headache Classification Committee of the International Headache Society (IHS). The international classification of headache disorders, 3rd edition (beta version). Cephalalgia 2013; 33: 629–808.
Hood D, Finkelstein M. Sensory processes and perception. In: Boff K, Kaufman L, Thomas J, editors. Handbook of perception and human performance. New York: John Wiley and Sons; 1986. p. 1–66.
Hurlbert AC, Ling Y. Biological components of sex differences in color preference. Curr Biol 2007; 17: R623–5.
Kawasaki A, Purvin VA. Photophobia as the presenting visual symptom of chiasmal compression. J Neuroophthalmol 2002; 22: 3–8.
Lamonte M, Silberstein SD, Marcelis JF. Headache associated with aseptic meningitis. Headache 1995; 35: 520–6.
Liveing E. On megrim, sick headache. Nijmegen: Arts & Boeve Publishers; 1873.
Lucas RJ, Douglas RH, Foster RG. Characterization of an ocular photopigment capable of driving pupillary constriction in mice. Nat Neurosci 2001; 4: 621–6.
Luck SJ, Hillyard SA. Electrophysiological correlates of feature analysis during visual search. Psychophysiology 1994; 31: 291–308.
Main A, Vlachonikolis I, Dowson A. The wavelength of light causing photophobia in migraine and tension-type headache between attacks. Headache 2000; 40: 194–9.
McCulloch DL, Marmor MF, Brigell MG, Hamilton R, Holder GE, Tzekov R, et al. ISCEV Standard for full-field clinical electroretinography (2015 update). Doc Ophthalmol 2015; 130: 1–12.
Mehta AD, Ulbert I, Schroeder CE. Intermodal selective attention in monkeys. I: distribution and timing of effects across visual areas. Cereb Cortex 2000a; 10: 343–58.
Mehta AD, Ulbert I, Schroeder CE. Intermodal selective attention in monkeys. II: physiological mechanisms of modulation. Cereb Cortex 2000b; 10: 359–70.
Miller RF, Dowling JE. Intracellular responses of the Muller (glial) cells of mudpuppy retina: their relation to b-wave of the electroretinogram. J Neurophysiol 1970; 33: 323–41.
Miura G, Wang MH, Ivers KM, Frishman LJ. Retinal pathway origins of the pattern ERG of the mouse. Exp Eye Res 2009; 89: 49–62.
Newman EA. Current source-density analysis of the b-wave of frog retina. J Neurophysiol 1980; 43: 1355–66.
Noseda R, Jakubowski M, Kainz V, Borsook D, Burstein R. Cortical projections of functionally identified thalamic trigeminovascular neurons: implications for migraine headache and its associated symptoms. J Neurosci 2011; 31: 14204–17.
Noseda R, Kainz V, Jakubowski M, Gooley JJ, Saper CB, Digre K, et al. A neural mechanism for exacerbation of headache by light. Nat Neurosci 2010; 13: 239–45.
Odom JV, Bach M, Brigell M, Holder GE, McCulloch DL, Tormene AP, et al. ISCEV standard for clinical visual evoked potentials (2009 update). Doc Ophthalmol 2010; 120: 111–9.
Palmer SE, Schloss KB. An ecological valence theory of human color preference. Proc Natl Acad Sci USA 2010; 107: 8877–82.
Paxinos G, Watson C. The rat brain in stereotaxic coordinates. 6th edn. Academic Press, Elsevier; 2008.
Penn RD, Hagins WA. Signal transmission along retinal rods and the origin of the electroretinographic a-wave. Nature 1969; 223: 201–4.
Quiroga RQ, Nadasdy Z, Ben-Shaul Y. Unsupervised spike detection and sorting with wavelets and superparamagnetic clustering. Neural Comput 2004; 16: 1661–87.
Robson JG, Frishman LJ. The rod-driven a-wave of the dark-adapted mammalian electroretinogram. Prog Retin Eye Res 2014; 39: 1–22.
Selby G, Lance JW. Observations on 500 cases of migraine and allied vascular headache. J Neurol Neurosurg Psychiat 1960; 23: 23–32.
Shirato S, Maeda H, Miura G, Frishman LJ. Postreceptoral contributions to the light-adapted ERG of mice lacking b-waves. Exp Eye Res 2008; 86: 914–28.
Strauss ED, Schloss KB, Palmer SE. Color preferences change after experience with liked/disliked colored objects. Psychon Bull Rev 2013; 20: 935–43.
Welty TE, Horner TG. Pathophysiology and treatment of subarachnoid hemorrhage. Clin Pharm 1990; 9: 35–9.
Zaidi FH, Hull JT, Peirson SN, Wulff K, Aeschbach D, Gooley JJ, et al. Short-wavelength light sensitivity of circadian, pupillary, and visual awareness in humans lacking an outer retina. Curr Biol 2007; 17: 2122–8.